Bispyridinium Dienes: Histone Deacetylase Inhibitors with Selective Activities

Carlos Pérez-Balado,[†] Angela Nebbioso,[‡] Paula Rodríguez-Graña,[†] Annunziata Minichiello,[‡] Marco Miceli,[‡] Lucia Altucci,*[,‡,§] and Ángel R. de Lera*[,†]

Departamento de Química Orgánica, Universidade de Vigo, Lagoas-Marcosende, 36310 Vigo, Spain, Dipartimento di Patologia Generale, Seconda Università degli Studi di Napoli, Vico L. de Crecchio 7 80138 Napoli, NOGEC, Naples Oncogenomic Center, CEINGE Biotecnologia Avanzata, Napoli, Italy

Received January 9, 2007

A novel synthetic route to the cyclostellettamines **1** using as the key step a microwave-mediated macrocyclic ring-closing metathesis of precursors bispyridinium dienes **10** followed by catalytic hydrogenation has been developed. The open-chain bispyridinium dienes **10** showed uniformly higher histone deacetylase (HDAC) inhibitory potency than the natural products. Diene **10b** inhibited HDAC1 and was inactive on HDAC4, whereas **10a** showed a weak inhibition of HDAC1 and a higher activity on HDAC4. Neither **10b** nor **10a** inhibited isoforms HDAC2 and HDAC3. Cell cycle analysis, cell differentiation, and apoptosis as well as evaluation of the acetylation status of H3 lysine tails, up-regulation of $p21^{WAF1/CIP1}$, and α-tubulin acetylation induced by the dienes **10** and cyclostellettamines **1** were also carried out on the human leukemia U937 cell line. These enzymatic and functional assays suggest that **10b** is a HDAC1-selective inhibitor and **10a** is a HDAC subclass IIa-selective inhibitor.

Introduction

While the genetic aberrations occurring in cancer are fairly well understood, we have only recently become aware of the epigenetic deregulation associated with cancer.[1] The deposition of epigenetic "marks" on chromatin, post-translational modifications of nucleosomal proteins and methylation of particular DNA sequences, is accomplished by enzymes often embedded in multi-subunit complexes.[2] The control of the enzymatic machinery implicated in the (un)packing of chromatin,[3] such as the reversible acetylation (HAT enzymes)/deacetylation (HDAC enzymes) of lysine residues,[4] the methylation/demethylation of histone lysine and arginine residues,[5] and the DNA methylation (DNMT enzymes)/demethylation[6] is an important step in the regulation of transcriptional events. As a consequence, chromating-remodeling enzymes, in particular HDACs and DNMTs, have recently emerged as new promising targets of the so-called "epigenetic drugs" for the treatment of cancer.[7,6a] Indeed, recent results indicate that epigenetic drugs may constitute an entirely novel type of anti-cancer therapy with unanticipated potential.[6a] Proof-of-principle comes from studies with histone deacetylase inhibitors, promising novel anti-cancer drugs, which are currently entering therapy.[7a,8] We and others have demonstrated that upon treatment with an HDAC inhibitor (HDACi), TRAIL (TNF-related apoptosis inducing ligand) is up-regulated and mediates acute apoptosis induced in both AML cells or patients blasts.[9a,b] Given the major interest in finding new therapies and the growing importance of epi-drugs for cancer treatment, there is a need for new molecules with epigenetic modulatory activities showing selectivity for particular families or members of the chromatin-modifying enzymes.[4b]

The cyclostellettamines are a growing family of macrocyclic bispyridinium alkaloids first isolated by Fusetani and co-workers in 1994 from the marine sponge *Haliclona sp.*[10a] Novel congeners have more recently been reported by the groups of Fusetani[10b] and Berlinck[10c] from other marine organisms. These natural products are endowed with interesting biological activities, among them the inhibition of binding of methyl quinuclidinyl benzylate to the muscarinic acetylcholinesterase receptors[10a] and, most notably, the inhibition of histone deacetylases.[10b] As HDAC inhibitors, the cyclostellettamine macrocyclic alkaloids are structurally unrelated to the already described inhibitors,[11] posing challenging questions about their mechanism of action. Structurally simple, the cyclostellettamines (termed A-L, **1a**−**l**, Figure 1) consist of two 3-alkylpyridinium units, connected by alkyl chains ranging from 10 to 14 carbons in length. These chains are fully saturated in most members of the family, except in two, namely dehydrocyclostellettamines D **2d** and E **2e**, which present one C−C double bond with *Z* geometry. Our interest in the anticancer activities of the epigenetic modulators[9a] led us to address the synthesis and determine the histone deacetylase inhibitory profile of this family of alkaloids. We present herein the synthesis, characterization, and biological evaluation of several members of the cyclostellettamine family of natural products. We confirm the reported micromolar HDAC inhibitory activity of most of the macrocyclic compounds, and most importantly we report that the open-chain precursors used as intermediates in the synthesis also exhibit differential HDAC inhibitory activities and could become promising leads for the development of more potent (sub)class-selective HDAC inhibitors.

Chemistry

The first total synthesis of cyclostellettamine C **1c** was accomplished by Fusetani and co-workers in 1996.[12a] Shortly after, the groups of Koomen and Baldwin independently reported analogous methodologies for the ring-closure based on the quaternization of the pyridine nitrogen.[12b,c] We considered a novel synthetic approach to these alkaloids using a ring-closing metathesis[13] of a bispyridinium diene precursor as the key transformation.

The synthesis began with the alkylation of the organolithium derived from the treatment of 3-methylpyridine **3** with LDA

* To whom correspondence should be addressed. Angel R. de Lera, Tel: +34-986-812316, Fax +34-986-811940, E-mail: qolera@uvigo.es; Lucia Altucci, Tel: +39081-566-7569, Fax: +39081-450-169, E-mail: lucia.altucci@unina2.it.

[†] Universidade de Vigo.

[‡] Seconda Università degli Studi di Napoli.

[§] CEINGE Biotecnologia Avanzata.

10.1021/jm070028m CCC: $37.00
Published on Web 04/21/2007

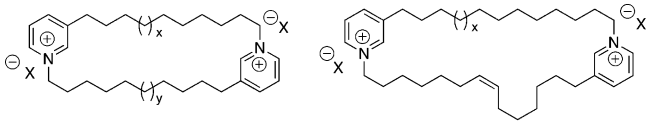

1a A x= 3, y= 3
1b B x= 3, y= 4
1c C x= 4, y= 4
1d D x= 3, y= 5
1e E x= 4, y= 5
1f F x= 5, y= 5
1g G x= 3, y= 2
1h H x= 1, y= 3
1i I x= 1, y= 4
1j J x= 1, y= 5
1l L x= 2, y= 5

2d dehydro D x= 1
2e dehydro E x= 2

Figure 1. Natural cyclostellettamines A-L (**1a**−**l**) and dehydroanalogues (**2d**, **2e**).

(Scheme 1).[14] For the C_{12} series, the THP-protected 11-bromoundecan-1-ol **4a** was used as alkylating agent, affording the alkylpyridine **5a** in 76% yield. In a similar manner, for the C_{13} series, bromide **4b** provided **5b**. Subsequent quaternization of the 3-alkylpyridines **5a**,**b** with 8-bromo-oct-1-ene furnished the pyridinium salts **6a** and **6b** in excellent yields. The THP group was removed with dilute HCl in methanol to give the free alcohols **7a** and **7b**. Activation of the alcohol function was easily effected by treatment with $SOCl_2$ in dichloromethane to yield the chloroalkylpyridinium chlorides **8a** and **8b**. The second pyridinium subunit was introduced by quaternisation of the 3-substituted pyridines **9a**, **9b**, and **9c** with chlorides **8a** and **8b** in the presence of 1.2 equiv of NaI to afford **10a**−**f** (Scheme 2). The 3-alkenyl pyridines **9a**−**c** were in turn prepared by alkylation of the lithiated 3-methylpyridine with the corresponding bromoalkenes (4-bromobut-1-ene for **9a**; 5-bromopent-1-ene for **9b** and 7-bromohept-1-ene for **9c**), as described for the synthesis of **5**. The alkylation of (pyrid-3-ylmethyl)lithium with 4-bromobut-1-ene, under the classical conditions (3 mol equiv of organolithium relative to the alkylating agent), gave a mixture of of **9a** and its regioisomer (*E*)-3-(pent-3′-en-1′-yl)-pyridine. Using equimolar amounts of both the organolithium and the alkylating agent resulted in lower yields (40%), but the expected terminal alkene **9a** was obtained as the exclusive product.

With a ready supply of the bispyridinium intermediates **10** at hand, attention was directed to the crucial olefin metathesis. Bispyridinium diene **10d**, selected as model system, was heated to reflux in dichloromethane in the presence of 5 mol % Grubbs second generation ruthenium catalyst **11**[15] (Scheme 3) to afford the expected macrocycle as a mixture of *E*/*Z* isomers. However, even after extended reaction times (up to 72 h), complete conversion of the starting material was not achieved, which implied a tedious separation of products. Pursuing a complete conversion of the open-chain diene, attention was turned to the acceleration effect of microwaves.[16] After some experimentation, the macrocyclisation was taken to completion in 20 min, working at constant microwave irradiation power (90 W). Moreover, the amount of catalyst **11** could be reduced to 2 mol %. At concentrations up to 0.02 M no oligomeric products, expected as the result of a competitive intermolecular cross-metathesis, were formed. Under the optimized conditions, no differences in reaction times or in conversions were noticed upon varying the ring size, and 29- to 33-membered bispyridinium macrocycles were efficiently assembled. The *E*/*Z* mixture of cyclic olefins was subjected without further purification to the hydrogenation of the C−C double bond catalyzed by Pd on charcoal to finally afford cyclostellettamines A **1a**, B **1b**, D **1d**, E **1e**, G **1g**, and the unnatural cyclostelletamine **12** in almost quantitative yield from the open-chain precursors **10b**, **10e**, **10c**, **10f**, **10a**, and **10d**, respectively. The spectroscopic data (^{1}H and ^{13}C NMR) of compounds **1a**,**b**,**d**,**e**,**g** were in full agreement with those reported for the natural materials.[10]

Scheme 1[a]

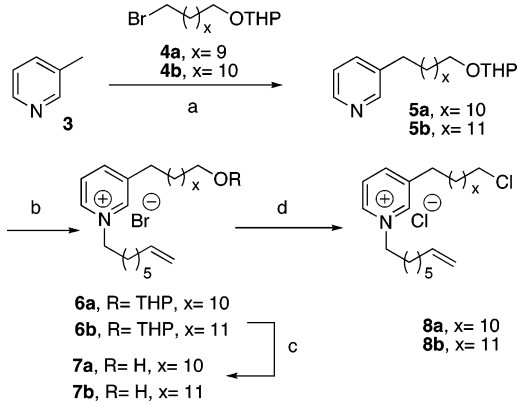

[a] Reagents and reaction conditions: (a) 1. LDA (3 equiv), THF, DMPU (3 equiv), 0 °C; 2. **4a** or **4b**, THF, −78 to 25 °C, 8 h, 70−76%. (b) 8-bromo-oct-1-ene, CH_3CN, reflux, 95−99%. (c) 0.5 M HCl, MeOH, 25 °C, 18 h, 82−87%. (d) $SOCl_2$, CH_2Cl_2, 25 °C, 3 h, 90−95%.

Scheme 2. Synthesis of the Open-Chain Precursors[a]

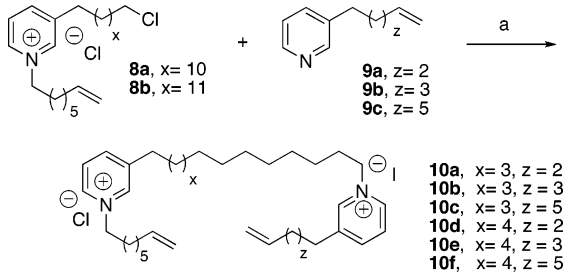

[a] Reagents and reaction conditions: (a) NaI (1.2 equiv), CH_3CN, reflux, 24 h, 55−70%.

This synthetic strategy provided access to the dehydrocyclostellettamines D **2d** and E **2e** as a mixture of *E*/*Z* isomers. Although their separation was possible by reversed phase HPLC on a C-30 column in a very small scale, the amphiphilic nature of cyclostellettamines makes impracticable the separation on a synthetically useful scale.

Biology

To assess the biological properties of the cyclostellettamines and their acyclic precursors, we first performed an analysis of cell cycle, differentiation, and apoptosis in the U937 acute myeloid leukemia cell line.

As shown in Figure 2A, some compounds were able to moderately increase differentiation after 30 h treatment, as assessed by the analysis of the expression of CD11c, a known marker of granulocytic differentiation. In particular, compounds **10a**−**d** showed around 30% increase in the expression of CD11c with compound **10b** being the most potent at 5 μM. The analysis of cell cycle, shown in Figure 2B, indicates that only particular compounds were able to induce accumulation of the cells in the G1 phase (black), with **10a** showing the highest efficiency. All open-chain bispyridinium dienes **10a**−**f** were able to induce apoptosis as measured by the percentage of active caspase 3 positive cells (Figure 2B, diffuse gray).

Since compounds **10a**−**f** showed a consistent biological activity, enzymatic assays were performed to evaluate their action on HDAC1 and HDAC4, considered as markers for Class I and Class II HDACs, respectively. Only diene **10b** used at 5 μM concentration was able to reduce the activity of HDAC1 (Figure 3). Compound **10a** on the contrary showed an inhibition of HDAC4 (see Figure 3) comparable to SAHA (**14**, Chart 1), whereas all other compounds showed either no (**10b**, **10c**, **10e**)

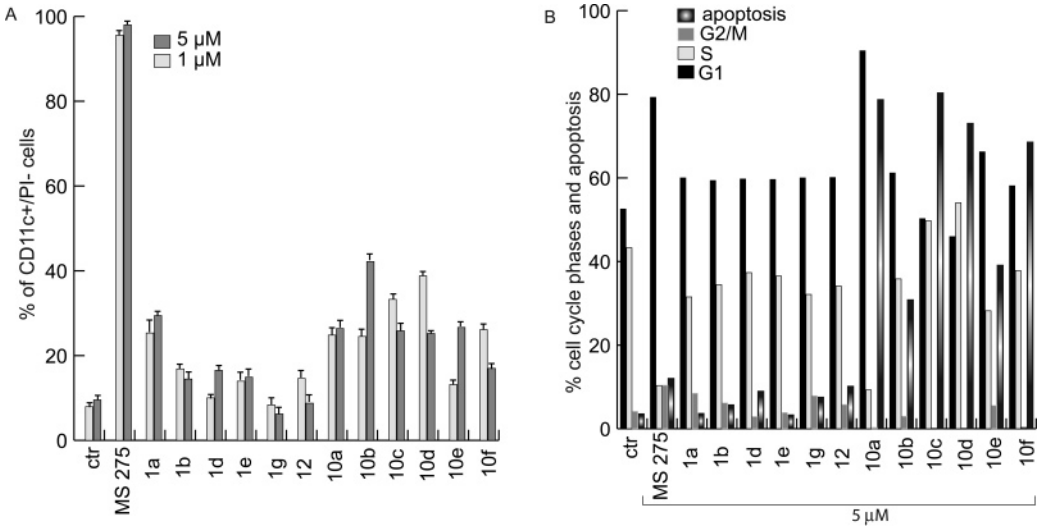

Figure 2. A. Differentiation analysis in U937 cells after 30 h treatment with the indicated compounds at 1−5 μM. The data shown represent the media of independent quadruplicates. B. Cell cycle analysis and apoptosis in U937 cells treated with the indicated compounds for 30 h. The data represent the media of independent duplicates.

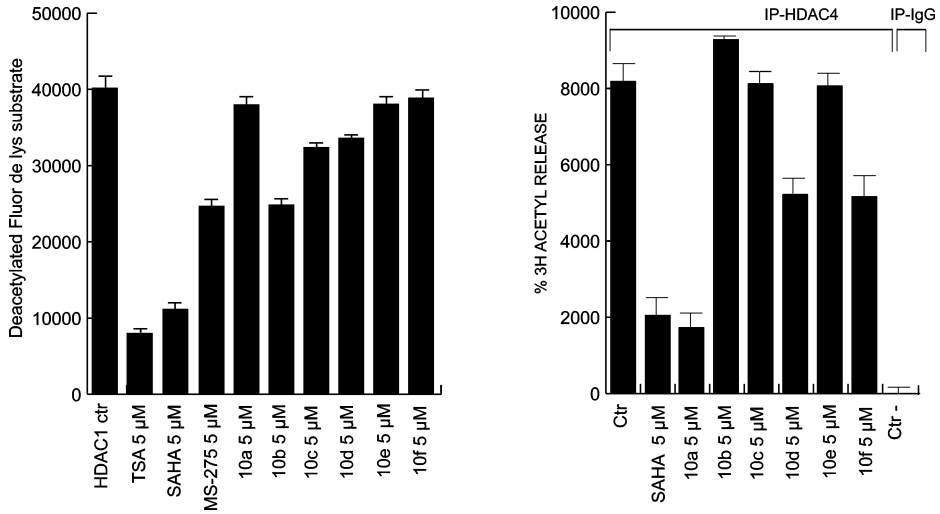

Figure 3. HDAC1 (left) and HDAC4 (right) assay with the indicated compounds.

Scheme 3. Synthesis of Cyclostellettamines by Ring-Closure Metathesis of the Bispyridinium Dienes **10** Followed by Hydrogenation of the Macrocyclic Olefins

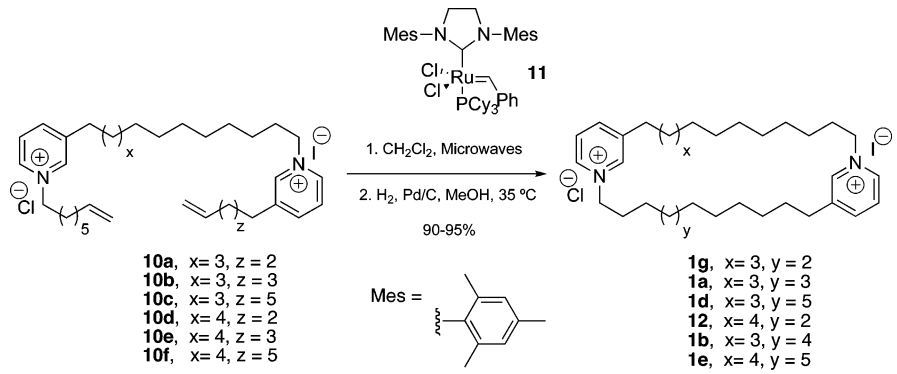

or low inhibition (**10d**, **10f**). IC_{50} values for HDAC1 are 1.88 μM for **10a** and 0.53 μM for **10b**, whereas IC_{50} values for HDAC4 are 0.54 μM for **10a** and >200 μM for **10b**.

Intrigued by the possible class specificity exerted by compounds **10a** and **10b**, the HDAC2 and HDAC3 enzymatic assays were also performed. As demonstrated in Figure 4, neither of the compounds showed inhibition in the *in vitro* HDAC2 and HDAC3 assays, whereas the reference SAHA (**14**, Chart 1) showed a good inhibition of both enzymes. The *o*-anilidobenzamide MS-275 (**15**, Chart 1), already characterized as a Class I HDAC-selective inhibitor,[9a] showed very low (ca. 30 times lower than HDAC1) activity on HDAC3,[17] indicating that its major targets are HDAC1 and HDAC2. The lack of activity of the bispyridinium diene **10a** in three of the four Class I HDAC enzymes, and its selective activity on HDAC4 renders it a promising Class II HDAC-selective inhibitor.

Chart 1. Representative Histone Deacetylase (HDAC) Inhibitors

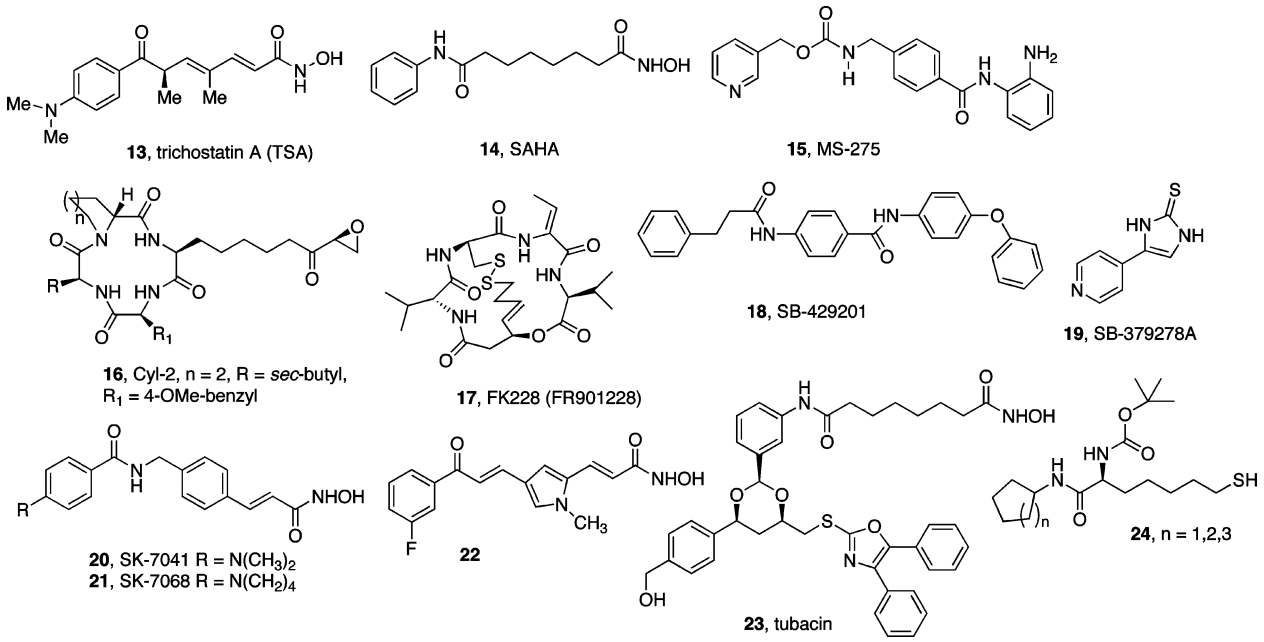

In order to assess the efficacy of the cyclostellettamines and their synthetic precursors on their putative molecular targets, their ability to alter acetylation levels at 5 μM concentration was tested. As shown in Figure 5, neither compound altered the extent of α-tubulin acetylation at 5 μM, whereas known HDAC inhibitors (such as SAHA **14** and MS-275 **15**) and compounds **1b**, **12**, and **10a**−**f** increased global histone H3 acetylation as assessed by Western Blot analysis using antibodies to these modifications. When the compounds were used at 1 μM, no modification of the acetylation levels was detected (data not shown). Interestingly, analog **10a** did not increase α-tubulin acetylation levels, thus confirming its unique features as a subclass IIa inhibitor.

Finally, the capacity of these compounds to induce overexpression of $p21^{WAF1/CIP1}$, a known target of class I- and pan-HDAC inhibitors, was verified. As shown in Figure 6 by Western Blot analysis, only compound **10b** was able to weakly induce $p21^{WAF1/CIP1}$ expression. Compound **10b** showed the most potent HDAC1 inhibition among the series of compounds and was inactive on HDAC2 and HDAC3. Given the very weak up-regulation of $p21^{WAF1/CIP1}$ by **10b** (compare to SAHA **14** and MS-275 **15** in Figure 6), it is tempting to suggest that inhibition of both HDAC1 and HDAC2 is required for $p21^{WAF1/CIP1}$ up-regulation.

Taken together, our findings show that compound **10b** displays the features of an HDAC1-selective inhibitor, and this activity correlates both with the histone H3 and α-tubulin acetylation levels and with the $p21^{WAF1/CIP1}$ induction. Moreover, compound **10a** show some Class IIa selectivity since it blocks HDAC4 activity without altering HDAC6-mediated α-tubulin deacetylation and does not modify HDAC1, HDAC2, and HDAC3 actions *in vitro*. Further investigations will be required to fully determine the inhibitory profile of bispyridinium diene **10a**.

Discussion

Acetylation/deacetylation reactions are critical to cell biological processes ranging from chromatin remodeling to DNA-binding activity, microtubule stabilization, protein−protein interactions, and small-molecule action.[8] In eukaryotic cells, the reversible acetylation of histones catalyzed by histone deacetylases (HDACs)/histone acetyl transferases (HATs) is involved in transcriptional regulation. The attachment of acetyl groups to the ϵ-amino group of lysine residues in the histone tails alters their charge and steric properties. As a consequence, both the internucleosomal and the histone−DNA interactions with the negatively charged phosphate backbone are destabilized. Unwinding of the chromatin structure by acetylation enables access of transcription factors and activation of gene expression.[1,7]

The eighteen known mammalian deacetylase enzymes are divided in two families, the histone deacetylases (eleven members) and the Sir2-like deacetylase or sirtuins (seven members).[18] HDACs appear to deacetylate the ϵ-acetylamido lysine by a nucleophilic attack of bound water to the Zn^{+2}-activated carbonyl group, creating a tetrahedral zinc alkoxide intermediate stabilized by enzyme residues which releases the acetyl group and the lysine products. Activation of the water molecule is caused by coordination to the Zn^{+2} (other metals such as Co and Cu have been suggested[19]) and the Asp-His charge relay system, although QM/MM studies suggest that the Zn^{+2} prefers to be tetrahedral, and water is instead activated by two His residues.[20] Sirtuins, related to the yeast protein Sir2p, function through a different mechanism requiring NAD^+ as a substrate and releasing *O*-acetyl-ADP ribose and nicotinamide as a consequence of acetyl transfer.[3]

HDACs are further subdivided into two classes according to their similarity in primary structure and size to *Sacharomyces cerevisiae* deacetylases: Class I HDACs (HDACs 1−3, 8, 11) are homologous to the yeast transcriptional regulator Rpd3 (*r*educed *p*otasssium *d*ependence 3) whereas Class II HDACs (HDACs 4−7, 9, 10) bear similarity to Hda1.[4b] HDAC11 is alternatively considered as a new Class IV.[7a] Differences between Class I and II HDACs are primarily noted in their size (with class II being from two to three times larger), their cellular localization, the conservation of sequence motifs in their catalytic domains, the identity of the protein−protein interaction complexes, and their tissue distribution. The catalytic domain of about 390 amino acids responsible for the deacetylation is highly conserved among all HDACs, in particular the residues lining the ligand-binding pocket. The crystal structures of the

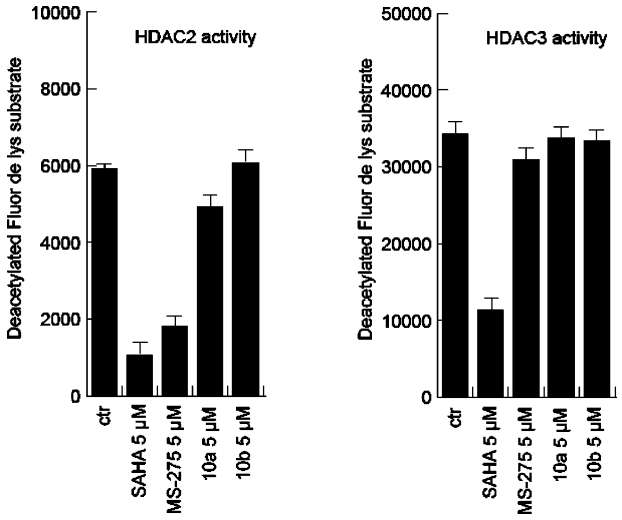

Figure 4. HDAC2 and HDAC3 enzymatic assays with the selected bis-pyridinium dienes **10a** and **10b**.

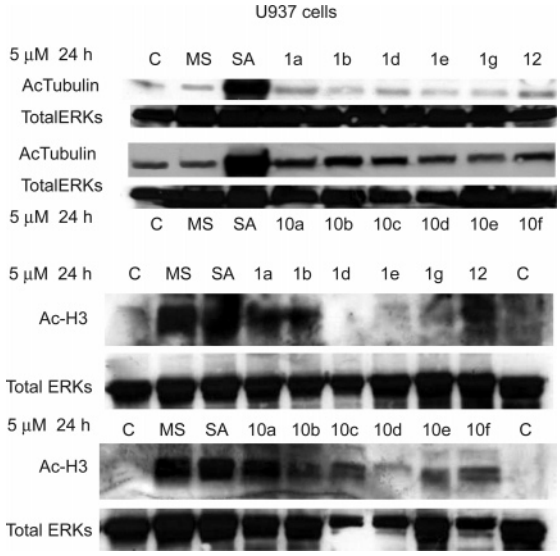

Figure 5. Western Blot analyses of histone H3 and α-tubulin acetylation carried out in U937 cells.

bacterial HDAC orthologue HDLP[21a] and the human HDAC8 in complexes with several natural (TSA, **13**) and synthetic inhibitors[21b,c] confirm the conserved nature of the aminoacids in contact with the ligand. Class I and Class II HDACs differ in the identity of the residues located at the rim of the entrance channel. In particular Tyr91 of HDLP changes its position upon ligand binding and is moreover poorly conserved among HDACs.[21a] These differences can be exploited for the design of class-selective HDAC inhibitors, although advances on the structure-based design of selective inhibitors have been scarce.[11] A recent crystal structure of HDAH (histone-deacetylase-like amidohydrolase from *Bordetella/alcaligens* strain FB188), a bacterial Class II HDAC homologue complexed to SAHA **14** and CypX, confirms the canonical fold of HDAC, the presence of the catalytic Zn^{+2} ion, and the divergences of the aminoacids of the binding pocket rim.[22] In addition, the aryl residues of Phe152 and Phe208 in the active site of HDAH are perfectly coplanar and separated by 7.8 Å, suggesting that π-stacking interaction with the ligand in this region might result in selective inhibition of Class II HDACs. The internal cavity used as an exit channel for the acetate leaving group after the deacetylation reaction[21b,c] also shows contrasting differences between Class I and Class II HDACs.[22]

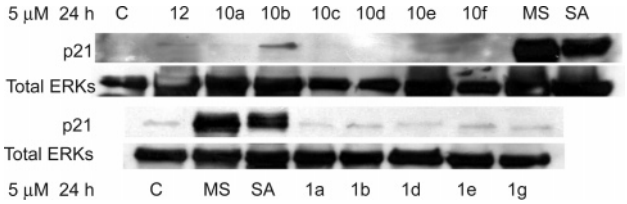

Figure 6. Western Blot analysis of $p21^{WAF1/CIP1}$ expression in U937 cells after treatment with the indicated compounds.

Most of the reported class-selective HDACs have been discovered after screening natural and synthetic products and chemical libraries,[11] with focus on differential inhibition of partially purified HDAC1 and HDAC6. These inhibitors (see Chart 1 for a selection) range from simple compounds (valproic acid, SAHA) to cyclic tetrapeptides called CHAPs, chimeras composed of the macrocyclic ring of trapoxin and the hydroxamic acid of TSA **13**. The majority of the described HDACs are pan-inhibitors acting on Class I and Class II enzymes (SAHA **14**, TSA **13**, PXD101, LBH589, LAQ824, etc.) or Class I and Class IIa (valproic acid, butyrate, trapoxin),[7b] and just a few show either Class- or member-selectivity. Notably, MS-275 **15** showed 40 000-fold selectivity for HDAC1 over HDAC6. MS-275 is a specific inhibitor of HDAC1, 2 and a weak inhibitor of HDAC3[17] (our unpublished data) whereas the IC_{50} for HDAC8 is much higher. However, the discrimination between HDAC1 and HDAC4 (Class II) is only modest. FK228 **17** (another reported HDAC1, 2-selective inhibitor) behaves similarly, with HDAC1/HDAC6 and HDAC1/HDAC4 values of 400 and 14, respectively.[11] Trapoxin analogue Cyl2 **16** exhibited 57 000-fold HDAC1/HDAC6 selectivity. Among the Class I member-selective inhibitors, structures have been reported for SB-429201 **18** which preferentially inhibits HDAC1, SB397278A **19**, an HDAC8-selective inhibitor,[23] and the HDAC1 and HDAC2- selective hydroxamic acids SK-7041 **20** and SK-7069 **21**.[24]

Class II-selective inhibitors are poorly represented. A family of aryloxopropenylpyrrolyl hydroxamic acids, exemplified by compound **22**, has been discovered by Mai et al.[25] A further subdivision within this Class is based on the identification of two deacetylase catalytic domains in Class IIb (HDAC6 and HDAC10) whereas only one is present in Class IIa (HDACs 4, 5, 7, 9).[26] Tubacin **23**, a member of a DOS-based 1,3-dioxane library, is a mammalian α-tubulin deacetylase specific inhibitor that selectively binds to the tubulin deacetylase catalytic domain of HDAC6 without altering the histone acetylation status, gene expression, or cell-cycle progression.[27a] Other HDAC6-selective inhibitors such as **24** have been built around the thiolate Zn^{+2}-chelating group.[27b]

Whereas some of the HDAC-selective inhibitors are endowed with a Zn^{+2}-chelating group (hydroxamic acid, thiols, mercaptoamides, trifluoromethylketones, etc.), thus pointing toward an inhibitory mechanism comprising binding site occupancy and competition with the natural substrate, others bear nonchelating functionalities, and alternative inhibition mechanisms should be entertained. For example, whereas modeling studies appear to support the occupancy of the exit channel for acetate as an inhibitory mechanism for the *o*-anilinobenzamide class represented by MS-275 **15**,[28] its exact nature remains controversial.[4b] Alternative mechanisms to the Zn^{+2}-competitive chelation such as the blocking of the entrance to the active site or to the acetate exit channel, the presence of additional binding sites with possible allosteric mode of actions and the inhibition of the interaction of HDACs with the histones should be considered in addition. In this regard, the macrocyclic bispyridinium salts

collectively known as cyclostellettamines **1** are intriguing HDACs, since they are structurally unrelated to any of the families of chemotypes known, and their structure cannot be dissected into the traditional metal binding-linker-rim components of most HDACs.[10b] Within the same family of natural products, their activities vary with the size of the macrocycle.[10b] These two aspects led us to consider the synthesis of the series of cyclostellettamines in order to contribute to their structure−activity relationship studies. For this purpose, we selected the ring-closing metathesis reaction to construct the macrocycle.[13] There are precedents on the ring-closing metathesis (RCM) of large diene-containing chains.[29] However, the use of pyridinium salts as substrates for the RCM was unprecedented. We showed that the RCM accelerated by microwaves is a highly efficient method for the formation of bispyridinium macrocycles ranging from 28 to 36 atoms in size. Combined with the catalytic hydrogenation, precursor dienes **10** are converted in high yields to the cyclostellettamines (the natural series **1**, and the unnatural congener **12**), thus completing a novel general approach to this family of natural products.

Characterization of these compounds confirmed the low inhibitory potential of the cyclostellettamines (in the micromolar range) with representative HDAC enzymes. However, the bis-diene precursors **10** displayed interesting activities, in particular **10b** and **10a**. The former is a HDAC1-selective inhibitor, and its activity correlates both with the histone H3 and α-tubulin acetylation levels and with the up-regulation of the cyclin-dependent kinase inhibitor $p21^{WAF1/CIP1}$, a well-known target of Class I HDAC inhibitors.[9a] Compound **10a** showed the unique profile of a subclass IIa-selective inhibitor, being able to block HDAC4 activity without altering HDAC6-mediated α-tubulin deacetylation and not modifying (if minimally) HDACs 1, 2, and 3 action *in vitro*. Compound **10b** is therefore a promising HDAC inhibitor showing a highly selective profile. Finally, compounds **10a**−**f** induced apoptosis in the myeloid monocytic U937 leukemia cell line. Given that only some of these compounds showed HDAC inhibitory properties, the induction of apoptosis might also be due to activities on different substrates. Indeed, both compounds **10a** and **10b** showed induction of apoptosis in the U937 cells, despite the fact that they target different HDAC enzymes.

Alkyl-substituted polyaminohydroxamic acids (PAHA) are a new type of HDACs[30a] built around the structures of spermidine and spermine, which are natural diamines known to inhibit yeast HDAC.[30b] The finding that the compounds with the highest activities in the PAHA series have a hydroxamic acid end and secondary amines in their chains suggests that the polyamine portion (which would be charged at physiological pH) on its own might retain HDAC inhibitory activity either by direct binding at the active site or by inhibition of the HDAC-chromatin recognition events. Whether this last mechanism is shared by the diene bispyridinium ions **10** remains to be demonstrated, but further experiments aimed to get a better understanding of the mechanism of HDAC inhibition by the synthetic open-chain diene precursors are already ongoing.

Summary and Conclusions

A new approach to the cyclostellettamines, macrocyclic bispyridinium natural products, has been developed based on the ring-closing metathesis of open-chain diene precursors. Compared to the previous syntheses, this approach is shorter and avoids the protection−deprotection sequence of one of the pyridine subunits. In addition, it shows the great versatility of the ring-closure metathesis to effect macrocyclisations. The HDAC inhibitory profile of both the cyclic bispyridinium alkaloids and the acyclic diene precursors was determined. Two of the open-chain bispyridinium dienes, namely **10b** and **10a**, displayed unique profiles, since they are selective inhibitors of HDAC1 and HDAC subclass IIa, respectively. Their contrasting selectivities are most intriguing, since they differ exclusively on one methylene carbon on the C3-alkyl chain of one pyridinium ring. The discovery of these novel chemotypes will pave the way for the development of new HDAC-selective inhibitors with promising application for cancer treatment.

Experimental Section

General. Reagents and solvents were purchased as reagent-grade and used without further purification unless otherwise stated. Solvents were dried according to standard methods and distilled before use. All reactions were performed in oven-dried or flame-dried glassware under an inert atmosphere of Ar unless otherwise stated. Chromatography refers to flash chromatography (FC) on SiO_2 60 (230−400 mesh) from Merck, head pressure of ca. 0.2 bar. TLC: UV_{254} SiO_2-coated plates from Merck, visualization by UV light (254 nm) or by coloring with 15% ethanolic phosphomolybdic acid solution. NMR spectra were recorded in a Bruker AMX400 (400.13 and 100.61 MHz for proton and carbon, respectively) spectrometer at 298 K with residual solvent peaks as internal reference and the chemical shifts are reported in δ [ppm], coupling constants J are given in hertz and the multiplicities assigned with DEPT experiments and expressed as follows: s = singlet, d = doublet, t = triplet, q = quartet, m = multiplet. COSY, HMBC, and HSQC methods were used to establish atom connectivities. Electronic impact ionization (EI) and fast atom bombardment (FAB) mass spectra were recorded on a VG-Autospec M instrument. Electrospray ionization (ESI) mass spectra were recorded on a Bruker APEX3 instrument. Infrared spectra (IR) were obtained on a JASCO FT/IR-4200 infrared spectrometer. Peaks are quoted in wave numbers (cm^{-1}) and their relative intensities are reported as follows: s = strong, m = medium, w = weak. Irradiation with microwaves was performed using a CEM DISCOVER apparatus.

General Procedure for the Preparation of the Open Chain Bispyridinium Salts. NaI (291 mg, 1.95 mmol) was added to a solution of 3-(13-chlorotridecyl)-1-(oct-7-enyl)pyridinium bromide **8b** (719 mg, 1.62 mmol) and 3-(oct-7-enyl)pyridine **9c** (369 mg, 1.95 mmol) in acetonitrile (10 mL). The resulting suspension was heated at reflux until disappearance of the starting material, as monitored by TLC. After completion of the reaction (usually 24 h), the solvent was removed under reduced pressure. The residue was purified by flash chromatography (90:10, CH_2Cl_2−MeOH) to afford 810 mg (69% yield) of 1-(oct-7-enyl)-3-(13-(3-(oct-7-enyl)-pyridinium-1-yl)tridecyl)pyridinium chloride iodide **10f** as a viscous yellow oil.

1-(Oct-7-enyl)-3-{12-[3-(pent-4-enyl)pyridinium-1-yl]dodecyl}-pyridinium Chloride Iodide (10a). ^{1}H NMR (400 MHz, CD_3OD) δ 9.06 (br s, 2H), 8.9−8.8 (m, 2H), 8.50 (d, J = 7.9 Hz, 2H), 8.04 (d, J = 6.9 Hz, 2H), 5.9−5.7 (m, 2H), 5.1−4.9 (m, 4H), 4.68 (t, J = 7.4 Hz, 4H), 3.0−2.9 (m, 4H), 2.2−2.1 (m, 2H), 2.1−2.0 (m, 6H), 1.9−1.8 (m, 2H), 1.8−1.7 (m, 2H), 1.5−1.2 (m, 22H) ppm. ^{13}C NMR (100 MHz, CD_3OD) δ 146.7 (2×), 145.6, 145.3, 143.4, 143.3, 139.8, 138.9, 129.0, 116.0, 115.0, 62.8 (2×), 34.6, 34.0, 33.5, 32.9, 32.5, 32.4, 31.5, 30.7, 30.5, 30.5 (3×), 30.4, 30.3, 30.0, 29.7, 29.5, 27.1, 26.9 ppm. IR (NaCl) ν 3017 (s), 2925 (s, C−H), 2853 (s, C−H), 1631 (m), 1504 (s), 1462 (s), 1153 (m), 911 (m), 731 (m), 689 (s). HRMS (ESI^+) m/z calcd for $C_{35}H_{56}IN_2^+$ 631.3483 (found 631.3490), $C_{35}H_{56}N_2^{2+}$ 252.2216 (found 252.2219).

3-(Hex-5-enyl)-1-{12-[1-(oct-7-enyl)pyridinium-3-yl]dodecyl}-pyridinium Chloride Iodide (10b). ^{1}H NMR (400 MHz, CD_3OD) δ 9.12 (br s, 2H), 8.9−8.8 (m, 2H), 8.48 (d, J = 8.0 Hz, 2H), 8.03 (dd, J = 8.0, 6.0 Hz, 2H), 5.9−5.7 (m, 2H), 5.1−4.9 (m, 4H), 4.66 (t, J = 7.5 Hz, 4H), 2.9−2.8 (m, 4H), 2.2−2.1 (m, 2H), 2.1−2.0 (m, 6H), 1.8−1.7 (m, 4H), 1.5−1.4 (m, 2H), 1.4−1.3 (m, 22H)

ppm. ^{13}C NMR (100 MHz, CD_3OD) δ 146.7 (2×), 145.7, 145.6, 145.3, 143.4, 143.3, 139.9, 139.5, 129.0, 115.3, 115.0, 62.9 (2×), 34.7, 34.4, 33.6, 33.4, 32.6, 32.5, 32.4, 31.6, 31.0, 30.7, 30.6, 30.6, 30.5 (2×), 30.4, 30.1 (2×), 29.8, 29.5, 29.4, 27.2, 27.0 ppm. IR (NaCl) ν 3015 (s), 2925 (s, C−H), 2853 (s, C−H), 1633 (m), 1504 (s), 1463 (m), 1153 (m), 909 (m), 688 (s). HRMS (ESI^+) *m/z* calcd for $C_{36}H_{58}IN_2^+$ 645.3639 (found 645.3630), $C_{36}H_{58}N_2^{2+}$ 259.2294 (found 259.2289).

General Procedure for Ring Closure Metathesis/Hydrogenation. Grubbs catalyst **11** (3.2 mg, 0.0036, 2 mol %) was added to a solution of 1-(oct-7-enyl)-3-{12-[3-(oct-7-enyl)pyridinium-1-yl]-dodecyl}pyridinium chloride iodide **10c** (134 mg, 0.188 mmol) in CH_2Cl_2 (6 mL), under argon. The resulting solution was irradiated with microwaves in a CEM-Discover apparatus in the constant power mode (90 W) for 20 min. The solvent was removed under reduced pressure. The macrocyclic product was dissolved in MeOH (6 mL), and 10% Pd on charcoal (21 mg, 10 mol %) was added. The mixture was heated at 32 °C under H_2 atmosphere (30 psi) for 48 h. The suspension was filtered over Celite and washed with MeOH (15 mL), and solvents were removed under reduced pressure. The residue was purified by semipreparative HPLC on a C-30 Develosil column (CH_3CN/H_2O:60/30, 0.1% TFA as eluent, isocratic mode) to afford 117 mg (91% yield) of cyclostellettamine D **1d** as a solid.

Cyclostellettamine D (1d). ^{1}H NMR (400 MHz, CD_3OD) δ 8.97 (br s, 2H, H2/2′), 8.86 (d, J = 5.9 Hz, 2H, H6/6′), 8.46 (d, J = 7.9 Hz, 2H, H4/4′), 8.03 (dd, J = 7.9, 5.9 Hz 2H, H5/5′), 4.62 (t, J = 7.5 Hz, 4H, H7/7′), 2.9−2.8 (m, 4H, H18/20′), 2.0−1.9 (m, 4H, H8/8′), 1.74 (t, J = 7.1 Hz, 4H, H17/19′), 1.5−1.2 (m, 36H, H9−16/9′-18′) ppm. ^{13}C NMR (100 MHz, CD_3OD) δ 146.7 (C4/4′), 145.9 (C3/3′), 145.3 (*C*2/2′), 143.4 (C6/6′), 129.0 (C5/5′), 63.0 (C7/7′), 33.6 (C18/20′), 32.6 (C8/8′), 31.7 (C17/19′), 30.7, 30.6, 30.5, 30.4, 30.3 (C10−15/10′-17′), 30.2 (C16/18′), 27.3 (C9/9′) ppm. IR (NaCl) ν 3020 (m), 2925 (s, C−H), 2852 (s, C−H), 1632 (m), 1505 (s), 1462 (m), 1155 (m), 692 (m). HRMS (ESI^+) *m/z* calcd for $C_{36}H_{60}IN_2^+$ 647.3796 (found 647.3789), $C_{36}H_{60}ClN_2^+$ 555.4439 (found 555.4434), $C_{36}H_{60}N_2^{2+}$ 260.2372 (found 260.2375).

Cell Lines and Cultures. The U937 cell line was cultured in RPMI with 10% fetal calf serum, 100 U/mL of penicillin, 100 μg/mL of streptomycin, 250 ng/mL of amphotericin-B, 10 mM HEPES, and 2 mM glutamine. U937 cells were kept at the constant concentration of 200 000 cells per milliliter of culture medium. Human breast cancer ZR-75.1 cells were propagated in DMEM medium supplemented with 10% fetal calf serum and antibiotics (100 U/mL of penicillin, 100 μg/mL of streptomycin, and 250 ng/mL of amphotericin-B).

Ligands and Materials. SAHA (kind gift of Merck) was dissolved in DMSO and used at 5 μM. MS-275 (kind gift from Schering AG) was dissolved in ethanol and used at 5 μM. Cyclostellettamines and related compounds were dissolved in DMSO and used at 1 or 5 μM.

Cell-Based Human HDAC4 Assay. Cells ZR75.1 cells were lysed in IP buffer (50 mM Tris-HCl at pH 7.0, 180 mM NaCl, 0.15% NP-40, 10% glycerol, 1.5 mM $MgCl_2$, 1 mM $NaMO_4$, and 0.5 mM NaF) with a protease inhibitor cocktail (Sigma), 1 mM DTT, and 0.2 mM PMSF for 10 min in ice and centrifuged at 13 000 rpm for 30 min. Then, 1000 μg amounts of extracts were diluted in IP buffer up to 1 mL and precleared by incubating with 20 μL of A/G plus Agarose (Santa Cruz) for 30 min to 1 h on a rocking table at 4 °C. Supernatants were transferred into a new tube, the antibodies (around 3 to 4 μg) were added, and IP was allowed to proceed overnight at 4 °C on a rocking table. The antibody used for HDAC4 was from Sigma. As the negative control, the same amounts of protein extracts were immunoprecipitated with the corresponding purified IgG (Santa Cruz). On the next day, 20 μL of A/G and Agarose (Santa Cruz) were added to each IP, and incubation was continued for 2 h. The beads were recovered by brief centrifugation and washed with cold IP buffer several times. The samples were than washed twice in PBS and resuspended in 20 μL of sterile PBS. The HDAC assay was carried out according to the supplier's instructions (Upstate). Briefly, samples immunoprecipitated with the HDAC4 and HDAC1 or with purified IgG were pooled separately to homogenize all samples. Then, 10 μL of the IP was incubated with a previously labeled 3H-Histone H4 peptide linked with streptavidine agarose beads (Upstate). In detail, 120 000 cpm of the H4-3H-acetyl-peptide was used for each tube and incubated in 1× HDAC buffer with 10 μL of the sample in the presence or absence of HDAC inhibitors with a final volume of 200 μL. Those samples were incubated overnight at 37 °C in slow rotation. On the next day, 50 μL of a quenching solution was added, and 100 μL of the samples was counted in duplicate after brief centrifugation in a scintillation counter. Experiments have been carried out in quadruplicate.

Fluorimetric HDAC1, 2, 3 Assays. The HDAC Fluorescent Activity Assay for HDAC1, 2, and 3 is based on the Fluor de Lys Substrate and Developer combination (BioMol AK-500) and has been carried out according to supplier's instructions and as previously reported.[31] First, the Fluor de Lys Substrate, which comprises an acetylated lysine side chain, has been incubated with purified recombinant HDAC1, 2, or 3 enzymes in presence or absence of the inhibitors. Briefly, for HDAC1, HDAC2, and HDAC 3, 100 ng, 25 ng, and 100 ng of recombinant proteins have been used per assay, respectively. Full length HDAC1 and 2 with C-terminal His tag were expressed using baculovirus expression systems; a complex of human HDAC3 full length with C-terminal tag and human NCOR2-N-terminal GST tag was coexpressed using baculovirus expression systems. Deacetylation sensitizes the substrate so that, in the second step, treatment with the developer produces a fluorophore. Fluorescence has been quantified with a TECAN Infinite M200 station.

IC_{50}. For compounds **10a** and **10b**, the IC_{50} was calculated using the *in vitro* enzymatic assay described above (Bio Mol). For HDAC 4 *in vitro* assay, amino acids 627−1085 with C-terminal GST tag were expressed using baculovirus expression systems. A 2 μg per assay has been used. The enzymatic incubation time chosen was 1−2 h. Four scalar concentrations in quadruplicate of the two compounds were tested for their enzymatic inhibition potential on HDAC1 and 4, and the relative IC_{50} was calculated using the TECAN Infinite M200 apparatus with the Magellan software.

Cell Cycle Analysis on U937 Cells. Cells (2.5×10^5) were collected and resuspended in 500 μL of hypotonic buffer (0.1% Triton X-100, 0.1% sodium citrate, 50 μg/mL of propidium iodide (PI), and RNAse A). Cells were incubated in the dark for 30 min. Samples were acquired on a FACS-Calibur flow cytometer using the Cell Quest software (Becton Dickinson) and analyzed with standard procedures using the Cell Quest software (Becton Dickinson) and the ModFit LT version 3 Software (Verity) as previously reported.[9a] All experiments were performed at least two times.

FACS Analysis of Apoptosis on U937 Cells. Apoptosis was measured with the active caspase 3 detection (B-Bridge), and samples were analyzed by FACS with Cell Quest technology (Becton Dickinson) as previously reported.[32]

Granulocytic Differentiation. Granulocytic differentiation was carried out according to the published procedure.[33] Briefly, U937 cells were harvested and resuspended in 10 μL of phycoerythrine-conjugated CD11c (CD11c-PE). Control samples were incubated with 10 μL of PE-conjugated mouse IgG1, incubated for 30 min at 4 °C in the dark, washed in PBS, and resuspended in 500 μL of PBS containing propidium iodide (0.25 μg/mL). Samples were analyzed by FACS with Cell Quest technology (Becton Dickinson). Propidium iodide positive cells have been excluded from the analysis.

Determination of α-Tubulin and Histone H3 Specific Acetylation. For α-tubulin, an amount of 50 μg of total protein extracts was separated on 10% polyacrylamide gels and blotted. Seventy four Western Blots were shown for acetylated α-tubulin (Sigma, 1:500 dilution), and total ERKs (Santa Cruz) were used to normalize for equal loading. For histone H3 specific acetylations, an amount of 100 μg of total protein extract was separated on 15% polyacrylamide gels and blotted.[34] Western Blots were shown for pan-acetylated histone H3 (Upstate), and total tubulin (Sigma) was used to normalize for equal loading.

Determination of p21$^{WAF1/CIP1}$ Induction in U937 Cells. Total protein extracts (100 μg) were separated on a 15% polyacrylamide gel and blotted as previously described.[9a] Western Blots were shown for p21 (Transduction Laboratories, 1:500 dilution), and total ERKs (Santa Cruz) were used to normalize for equal loading.

Acknowledgment. The authors are grateful to the European Union (EPITRON, LSHC-CT-2005-518417), Xunta de Galicia (visiting scientist fellowship to C.P.B.), the Spanish Ministerio de Educación y Ciencia (SAF04-07131, FEDER) and the Italian Ministero dell Istruzione Università e Ricerca (PRIN 2006052835_003) for financial support. A.N., M. M. and A. M. are supported by EU (LSHC-CT-2005-518417). We specially thank Prof. Nobuhiro Fusetani and Dr. Naoya Oku for insightful discussions on separation of dehydrocyclostellettamines.

Supporting Information Available: Experimental procedures, analytical and spectral characterization data for compounds **4**−**8b**, **9a**−**c**, **10c**−**f**, **1a**, **1b**, **1e**, **1g**, and **12**. This material is available free of charge via the Internet at http://pubs.acs.org.

References

(1) (a) Baylin, S. B.; Ohm, J. E. Epigenetic Gene Silencing in Cancer-A Mechanism for Early Oncogenic Pathway Addiction? *Nature Rev. Cancer* **2006**, *6*, 107−116. (b) Yoo, C. B.; Jones, P. A. Epigenetic therapy of cancer: past, present and future. *Nat. Rev. Drug Discovery* **2006**, *5*, 37−50.

(2) Marmorstein, R. Protein Modules that Manipulate Histone Tails for Chromatin Regulation. *Nat. Rev. Mol. Cell Biol.* **2001**, *2*, 422−432.

(3) Biel, M.; Wascholowski, V.; Giannis, A. Epigenetics-An Epicenter of Gene Regulation: Histones and Histone-Modifying Enzymes. *Angew. Chem., Int. Ed.* **2005**, *44*, 3186−3216.

(4) (a) Kouzarides, T. Acetylation: a regulatory modification to rival phosphorylation. *EMBO J.* **2000**, *19*, 1176−1179. (b) Mai, A.; Massa, S.; Rotili, D.; Cerbara, I.; Valente, S.; Pezzi, R.; Simeoni, S.; Ragno, R. Histone Deacetylation in Epigenetics: An Attractive Target for Anticancer Therapy. *Med. Res. Rev.* **2005**, *25*, 261−309.

(5) (a) Bannister, A. J.; Kouzarides, T. Reversing histone methylation. *Nature* **2005**, *436*, 1103−1106. (b) Bedford, M. T.; Richard, S. Arginine Methylation: An Emerging Regulator of Protein Function. *Cell* **2005**, *18*, 263−272. (c) Jenuwein, T. The epigenetic magic of histone lysine methylation. *FEBS J.* **2006**, *273*, 3121−3135.

(6) (a) Das, P. M.; Singal, R. DNA methylation and cancer. *J. Clin. Oncol.* **2004**, *22*, 4632−4642. (b) Schneider, J.; Shilatifard, A. Histone Demethylation by Hydroxylation: Chemistry in Action. *ACS Chem. Biol.* **2006**, *1*, 75−81.

(7) (a) Minucci, S.; Pelicci, P. G. Histone deacetylase inhibitors and the promise of epigenetic (and more) treatments for cancer. *Nat. Rev. Cancer* **2006**, *6*, 38−51. (b) Bolden, J. E.; Peart, M. J.; Johnstone, R. W. Anticancer activities of histone deacetylase inhibitors. *Nat. Rev. Drug Discovery* **2006**, *5*, 769−784.

(8) Grozinger, C. M.; Schreiber, S. L. Deacetylase Enzymes: Biological Functions and the Use of Small Molecule Inhibitors. *Chem. Biol.* **2002**, *9*, 3−16.

(9) (a) Nebbioso, A.; Clarke, N.; Bontempo, P.; Volz, E.; Alvarez, R.; Schiavone, E. M.; Weisz, A.; Bresciani, F.; de Lera, A. R.; Gronemeyer, H.; Altucci, L. Tumor-selective action of HDAC Inhibitors involves TRAIL induction in acute myeloid leukemia cells. *Nat. Med.* **2005**, *11*, 77−84. (b) Insinga, A.; Monestiroli, S.; Ronzoni, S.; Gelmetti, V.; Marchesi, F.; Viale, A.; Altucci, L.; Nervi, C.; Minucci, S.; Pelicci, P. G. Inhibitors of histone deacetylases induce tumor-selective apoptosis through activation of the death receptor pathway. *Nat. Med.* **2005**, *11*, 71−76.

(10) (a) Fusetani, N.; Asai, N.; Matsunaga, S.; Honda, K.; Yasumuro, K. Bioactive marine metabolites. 59. Cyclostellettamines A-F, pyridine alkaloids which inhibit binding of methyl quinuclidinyl benzylate (QNB) to muscarinic acetylcholine receptors, from the marine sponge, *Stelletta maxima*. *Tetrahedron Lett.* **1994**, *35*, 3967−3970. (b) Oku, N.; Nagai, K.; Shindoh, N.; Terada, Y.; Van Soest, R. W. M.; Matsunaga, S.; Fusetani, N. Three new cyclostellettamines, which inhibit histone deacetylase, from a marine sponge of the genus *Xestospongia*. *Bioorg. Med. Chem. Lett.* **2004**, *14*, 2617−2620. (c) De Oliveira, J. H. H. L.; Grube, A.; Koeck, M.; Berlinck, R. G. S.; Macedo, M. L.; Ferreira, A. G.; Hajdu, E. Ingenamine G and cyclostellettamines G-I, K, and L from the new Brazilian species of marine sponge *Pachychalina* sp. *J. Nat. Prod.* **2004**, *67*, 1687−1689.

(11) Miller, T. A.; Witter, D. J.; Belvedere, S. Histone Deacetylase Inhibitors. *J. Med. Chem.* **2003**, *46*, 5097−5114.

(12) (a) Anan, H.; Seki, N.; Noshiro, O.; Honda, K.; Yasumuro, K.; Ozasa, T.; Fusetani, N. Total synthesis of cyclostellettamine C, a bispyridinium macrocyclic alkaloid having muscarinic acetylcholine receptor antagonistic activity. *Tetrahedron* **1996**, *52*, 10849−10860. (b) Baldwin, J. E.; Spring, D. R.; Atkinson, C. E.; Lee, V. Efficient synthesis of the sponge alkaloids cyclostellettamines A-F. *Tetrahedron* **1998**, *54*, 13655−13680. (c) Grube, A.; Timm, C.; Koeck, M. Synthesis and mass spectrometric analysis of cyclostellettamines H, I, K and L. *Eur. J. Org. Chem.* **2006**, 1285−1295.

(13) Nicolaou, K. C.; Bulger, P. G.; Sarlah, D. Metathesis Reactions in Total Synthesis. *Angew. Chem., Int. Ed.* **2005**, *44*, 4490−4527.

(14) Davies-Coleman, M. T.; Faulkner, D. J.; Dubowchik, G. M.; Roth, G. P.; Polson, C.; Fairchild, C. J. A new EGF-active polymeric pyridinium alkaloid from the sponge *Callyspongia fibrosa*. *J. Org. Chem.* **1993**, *58*, 5925−5930.

(15) Trnka, T. M.; Grubbs, R. H. The development of L_2X_2Ru:CHR olefin metathesis catalysts: an organometallic success story. *Acc. Chem. Res.* **2001**, *34*, 18−29.

(16) Nosse, B.; Schall, A.; Jeong, B. W.; Reiser, O. Optimization of ring-closing metathesis: Inert gas sparging and microwave irradiation. *Adv. Synth. Cat.* **2005**, *347*, 1869−1874.

(17) Inoue, S.; Mai, A.; Dyer, M. J.; Cohen, G. M. Inhibition of histone deacetylase class I but not class II is critical for the sensitization of leukemic cells to tumor necrosis factor-related apoptosis-inducing ligand-induced apoptosis. *Cancer Res.* **2006**, *66*, 6785−6792.

(18) de Ruijter, A. J. M.; ven Gennip, A. H.; Caron, H. N.; Kemp, S.; Kuilenburg, A. B. P. Histone deacetylases (HDACs). Characterization of the classical HDAC family. *Biochem. J.* **2003**, *370*, 737−749.

(19) Gantt, S. L.; Gattis, S. G.; Fierke, C. A. Catalytic Activity and Inhibition of Human Histone Deacetylase 8 Is Dependent on the Identity of the Active Site Metal Ion. *Biochemistry* **2006**, *45*, 6170−6178.

(20) Corminboeuf, C.; Hu, P.; Tuckerman, M. E.; Zhang, Y. Unexpected Deacetylation Mechanism Suggested by a Density Functional Theory QM/MM Study of Histone-Deacetylase-Like Protein. *J. Am. Chem. Soc.* **2006**, *128*, 4530−4531.

(21) (a) Finnin, M. S.; Donigian, J. R.; Cohen, A.; Richon, V. M.; Rifkind, R. A.; Marks, P. A.; Pavletich, N. P. Structures of a Histone Deacetylase Homologue Bound to the TSA and SAHA inhibitors. *Nature* **1999**, *401*, 188−193. (b) Vannini, A.; Volpari, C.; Filocamo, G.; Casavola, E. C.; Brunetti, M.; Renzoni, D.; Chakravarty, P.; Paolini, C.; De Francesco, R.; Gallinari, P.; Steinkühler, C.; Di Marco, S. Crystal structure of a eukatyotic zinc-dependent histone deacetylase, human HDAC8, complexed with a hydroxamic acid inhibitor. *Proc. Natl. Acad. Sci. U.S.A.* **2004**, *101*, 15064−15069. (c) Somoza, J. R.; Skene, R. J.; Katz, B. A.; Mol, C.; Ho, J. D.; Jennings, A. J.; Luong, C.; Arvai, A.; Buggy, J. J.; Chi, E.; Tang, J.; Sang, B.-C.; Verner, E.; Wynands, D. R.; Snell, G.; Navre, M.; Knuth, M. W.; Swanson, R. V.; McRee, D. E.; Tari, L. W. Structural Snapshots of Human HDAC8 Provide Insights Into the Class I Histone Deacetylase. *Structure* **2004**, *12*, 1325−1334.

(22) Nielsen, T. K.; Hildmann, C.; Dickmanns, A.; Schwienhorst, A.; Ficner, R. Crystal structure of a Bacterial Class 2 Histone Deacetylase Homologue. *J. Mol. Biol.* **2005**, *354*, 107−120.

(23) Hu, E.; Dul, E.; Sung, C.-M.; Chen, Z.; Kirkpatrick, R.; Zhang, G.-F.; Johanson, K.; Liu, R.; Lago, A.; Hofmann, G.; Macarron, R.; Perez, P.; Krawiec, J.; Winkler, J.; Jaye, M. Identification of Novel Isoform-Selective Inhibitors within Class I Histone Deacetylases. *J. Pharmacol. Exp. Ther.* **2003**, *307*, 720−728.

(24) Park, J.-H.; Jung, Y. J.; Kim, T. Y.; Kim, S. G.; Jong, H.-S.; Lee, J. W.; Kim, D.-K.; Lee, J.-S.; Kim, N. K.; Kim, T.-Y.; Bang, Y.-J. Class I Histone Deacetylase-Selective Novel Synthetic Inhibitors Potently Inhibit Human Tumor Proliferation. *Clin. Cancer Res.* **2004**, *10*, 5271−5281.

(25) (a) Mai, A.; Massa, S.; Pezzi, R.; Rotili, D.; Loidl, P.; Brosch, G. Discovery of (Aryloxopropenyl)pyrrolyl Hydroxamides as Selective Inhibitors of Class IIa Histone Deacetylase Homologue HD1-A. *J. Med. Chem.* **2003**, *46*, 4826−4829. (b) Mai, A.; Massa, S.; Valente, S.; Simeoni, S.; Ragno, R.; Bottoni, P.; Scatena, R.; Brosch, G. Aroyl-pyrrolyl hydroxyamides: influence of pyrrole C4-phenylacetyl substitution on histone deacetylase inhibition. *ChemMedChem* **2006**, *1*, 225−237.

(26) (a) Grozinger, C. M.; Hassig, C. A.; Schreiber, S. L. Three proteins define a class of human histone deacetylases related to yeast Hda1p.

Proc. Natl. Acad. Sci. U.S.A. **1999**, *96*, 4868−4873. (b) Fischle, W.; Kiermer, V.; Dequiedt, F.; Verdin, E. The emerging role of class II deacetylases. *Biochem. Cell Biol.* **2001**, *79*, 337−348. (c) Bertos, N. R.; Wang, A. H.; Yang, X. Y. Class II Histone Deacetylases: Structure, Function and Regulation. *Biochem. Cell Biol.* **2001**, *79*, 243−252.

(27) (a) Haggarty, S. J.; Koeller, K. M.; Grozinger, C. M.; Schreiber, S. L. Domain-selective Small-molecule Inhibitor of Histone Deacetylase 6 (HDAC-6)-mediated Tubulin Acetylation. *Proc. Natl. Acad. Sci. U.S.A.* **2003**, *100*, 4389−4394. (b) Suzuki, T.; Kouketsu, A.; Itoh, Y.; Hisakawa, S.; Maeda, T.; Yoshida, M.; Nakagawa, H.; Miyata, N. Highly Potent and Selective Histone Deacetylase 6 Inhibitors Designed Based on a Small-Molecule Substrate. *J. Med. Chem.* **2006**, *49*, 4809−4812.

(28) Wang, D.-F.; Helquist, P.; Wiech, N. L.; Wiest, O. Toward Selective Histone Deacetylase Inhibitor Design: Homology Modeling, Docking Studies, and Molecular Dynamics Simulations of Human Class I Histone Deacetylase. *J. Med. Chem.* **2005**, *48*, 6936−6947.

(29) Ibrahim, Y. A.; John, E. Efficient synthesis of 18−40 membered macrocyclic polyoxadiamides and polyoxatetraamides via ring closing metathesis. *Tetrahedron Lett.* **2006**, *62*, 1001−1014.

(30) (a) Varghese, S.; Gupta, D.; Baran, T.; Jiemjit, A.; Gore, S. D.; Casero, R. A.; Woster, P. M. Alkyl-Substituted Polyhydroxamic Acids: A Novel Class of Targeted Histone Deacetylase Inhibitors. *J. Med. Chem.* **2005**, *48*, 6350−6365. (b) Vu, Q. A.; Zhang, D.; Chroneos, Z. C.; Nelson, D. A. Polyamines inhibit the yeast histone deacetylase. *FEBS Lett.* **1987**, *220*, 79−83.

(a) Kapustin, G. V.; Fejér, G.; Gronlund, J. L.; McCafferty, D. G.; Seto, E.; Etzkorn, F. A. Phosphorus-Based SAHA Analogues as Histone Deacetylase Inhibitors. *Org. Lett.* **2003**, *5*, 3053−3056. (b) Gurvich, N.; Tsygankova, O. M.; Meinkoth, J. L.; Klein, P. S. Histone Deacetylase Is a Target of Valproic Acid-Mediated Cellular Differentiation. *Cancer Res.* **2004**, *64*, 1079−1086.

(a) Mai, A.; Massa, A.; Rotili, D.; Simeoni, S.; Ragno, R.; Botta, G.; Nebbioso, A.; Miceli, M.; Altucci, L.; Brosch, G. Synthesis and Biological Properties of Novel, Uracil-Containing Histone Deacetylase Inhibitors. *J. Med. Chem.* **2006**, *49*, 6046−6056.

Altucci, L.; Rossin, A.; Raffelsberger, W.; Reitmair, A.; Chomienne, C.; Gronemeyer, H. Retinoic acid-induced apoptosis in leukemia cells is mediated by paracrine action of tumor-selective death ligand TRAIL. *Nat. Med.* **2001**, *7*, 680−686.

Mai, A.; Massa, A.; Pezzi, R.; Simeoni, S.; Rotili, D.; Nebbioso, A.; Scognamigliio, A.; Altucci, L.; Loidl, P.; Brosch, G. Class II (IIa)-Selective Histone Deacetylase Inhibitors. 1. Synthesis and Biological Evaluation of Novel (Aryloxopropenyl)pyrrolyl Hydroxamides. *J. Med. Chem.* **2005**, *48*, 3344−3353.

JM070028M